Robust Beamforming Technique with Sidelobe Suppression Using Sparse Constraint on Beampattern

Ying Zhang [1], Huapeng Zhao [1], Joni Polili Lie [2], Boon Poh Ng [1], and Qun Wan [3]

[1] School of Electrical and Electronic Engineering
Nanyang Technological University, Singapore, 639798, Singapore
zhangy@ntu.edu.sg, zh0044ng@ntu.edu.sg, ebpng@ntu.edu.sg

[2] Temasek Laboratories@Nanyang Technological University
Nanyang Technological University, Singapore, 639798, Singapore
JoniLie@ntu.edu.sg

[3] Department of Electronic Engineering
University of Electronic Science and Technology of China, Chengdu, 610066, China
wanqun@uestc.edu.cn

Abstract ─ In this paper, we propose two beamforming algorithms which impose sparse constraint on beampattern to suppress the sidelobe level and enhance robustness of the beamformer against steering vector error. The sparse constraint is given by an l_p-norm, where $p \leq 2$ holds. It is shown that the proposed algorithms can be solved using iterative algorithm. Computer simulations show that the proposed algorithms not only yield lower sidelobe level than that of the conventional beamformer, but also show better robustness against steering vector error than the conventional beamformers.

Index Terms ─ Beamforming, robust, sidelobe, sparse, steering vector error.

I. INTRODUCTION

Adaptive beamforming is an important research topic in array signal processing. It is to enhance the source from the desired direction, while suppressing the background noise and all the interference from other directions. A representative beamformer is the minimum variance and distortionless response (MVDR) beamformer [1] which casts deep nulls in the directions of strong interferences and at the meantime guarantees the desired signal distortionless. One of the disadvantages of the MVDR beamformer is its high sidelobe level which results in significant performance degradation in case of unexpected interference or increase of the noise power [2]. In practice, look direction mismatch due to imperfect array occurs. In such case, the signal of interest (SOI) will be mistaken as interference and the performance of the MVDR beamformer is known to degrade dramatically [3].

There has been much effort dedicated to design robust beamforming algorithms against imperfect array [4]. To address the uncertainty of the steering vector and the direction-of-arrival (DOA) of SOI, a set of unity-gain constraints for neighboring directions of the nominal look direction can be imposed [5]. Besides, the derivative of the array output can be imposed to zero at the desired look angle, which is called the derivative mainbeam constraints [6-8]. Some regularization methods [9, 10] are also proposed to enhance the robustness of the MVDR beamformer against steering vector error [11]. Beamformers using eigenvalue thresholding methods to achieve robustness have also been discussed [12].

In this paper, we propose two new beamforming algorithms which are robust against look direction mismatch and steering vector error. Besides, the achieved beampatterns have lower sidelobe level compared with the MVDR beamformer. Sidelobe suppression is realized via imposing a sparse constraint on beampattern with

respect to potential interference directions. Due to imperfect knowledge of the array, the presumed directions of SOI maybe vary from the real ones, thereby causes cancelation of SOI. To solve this problem, mainlobe control is considered. Instead of maintaining distortionless response on one look direction, the proposed algorithm attempts to maintain distortionless response on a wide angular range so that sources impinging on the array from nearby directions of look direction can be retained. The two algorithms may be solved iteratively. The validity and advantages of the new algorithms are verified via computer simulations.

II. ALGORITHM I: SIDELOBE SUPPRESSION WITH SPARSE CONSTRAINT ON BEAMPATTERN

The mathematical formulation of the MVDR beamformer is given by

$$\min_{\mathbf{w}} \mathbf{w}^H\mathbf{R}\mathbf{w}, \quad (1a)$$

$$\text{subject to } \mathbf{w}^H\mathbf{a}(\theta_0) = 1, \quad (1b)$$

where $\mathbf{R}$ is the covariance matrix of data, and $\mathbf{w}$ denotes the beamforming vector. From the perspective of beampattern, it is observed from (1b) that there is only an explicit constraint on the look direction, i.e. θ_0, while no constraint is imposed on the directions of interference. To repair this drawback, we propose the following optimization problem with an additional constraint on the sparsity of the beampattern with respect to potential interference directions:

$$\min_{\mathbf{w}} \mathbf{w}^H\mathbf{R}\mathbf{w}/2\,, \quad (2a)$$

$$\text{subject to } \mathbf{w}^H\mathbf{a}(\theta_0) = 1\,, \quad (2b)$$

$$\|\mathbf{w}^H\mathbf{A}\|_p^p < \varepsilon, \quad (2c)$$

where $\mathbf{A}$ is an $L \times N$ matrix which consists of steering vectors in the angular range which contains all the possible interference directions, L is the number of sensors, and N denotes the number of spatial samplings over the angular range with respect to the interference. It is noticed that we have imposed (2c) to the original formulation of the MVDR beamformer (1).

In (2c), $\|\mathbf{x}\|_p = (\sum_i |x_i|^p)^{1/p}$ is the l_p-norm of the vector $\mathbf{x}$. When p < 2, the l_p-norm can be defined as "dispersion" of the super-Gaussian distributions. When p≤1, the l_p-norm can be interpreted as the diversity measurement [13]. The smaller the value of $\|\mathbf{x}\|_p^p$, the sparser the $\mathbf{x}$ is, which means the number of trivial entries in $\mathbf{x}$ is larger. For beamforming, the smaller the value of $\|\mathbf{w}^H\mathbf{A}\|_p^p$, the lower the sidelobe level, since most of the entries in $\mathbf{w}^H\mathbf{A}$ are forced to some trivial values. For our sparse constraint, we require the value of p to be smaller than 2.

To derive the solution of (2), the Lagrange multiplier technique is used:

$$\mathrm{J}(\mathbf{w}) = \frac{\mathbf{w}^H\mathbf{R}\mathbf{w}}{2} + \lambda\|\mathbf{w}^H\mathbf{A}\|_p^p + \gamma(\mathbf{w}^H\mathbf{a}(\theta_0) - 1), \quad (3)$$

where λ and γ are Lagrange multipliers.

Define $\bar{\mathbf{A}} = [\mathbf{A}|\alpha\mathbf{a}(\theta_0)]$, $\mathbf{d}^T = [\mathbf{0}^T|\alpha\mathbf{1}]$, where $\alpha = \gamma/\lambda$. (3) is equivalent to

$$\mathrm{J}(\mathbf{w}) = \frac{\mathbf{w}^H\mathbf{R}\mathbf{w}}{2} + \lambda\|\,\bar{\mathbf{A}}^H\mathbf{w} - \mathbf{d}^*\|_p^p, \quad (4)$$

where * denotes complex conjugate.

Calculating the gradient of $\mathrm{J}(\mathbf{w})$ with respect to $\mathbf{w}$, we have

$$\nabla_{\mathbf{w}}\mathrm{J}(\mathbf{w}) = \mathbf{R}\mathbf{w} + \tilde{\lambda}\,\bar{\mathbf{A}}\boldsymbol{\Pi}(\boldsymbol{w})(\,\bar{\mathbf{A}}^H\mathbf{w} - \mathbf{d}^*), \quad (5)$$

where $\tilde{\lambda} = \lambda\mathrm{p}$, and $\boldsymbol{\Pi}(\boldsymbol{w})$ is given by $\boldsymbol{\Pi}(\boldsymbol{w}) = \mathrm{diag}\{|(\,\bar{\mathbf{A}}^H\mathbf{w} - \mathbf{d}^*)_1|^{p-2}, \ldots, |(\,\bar{\mathbf{A}}^H\mathbf{w} - \mathbf{d}^*)_N|^{p-2}\}$.

Equating (5) to zero, and using the gradient factorization approach [13], the update formula of $\mathbf{w}$ is given by

$$\mathbf{w}(i+1) = \tilde{\lambda}\left(\mathbf{R} + \tilde{\lambda}\,\bar{\mathbf{A}}\boldsymbol{\Pi}(\mathbf{w}(i))\,\bar{\mathbf{A}}^H\right)^{-1}\bar{\mathbf{A}}\boldsymbol{\Pi}(\mathbf{w}(i))\mathbf{d}^*, \quad (6)$$

where i denotes the iteration index.

III. ALGORITHM II: SIDELOBE SUPPRESSION WITH ROBUSTNESS CONSIDERATION

Notice that the above formulation is proposed under the assumption that the real steering vector is known. When the presumed steering vector is used instead of the real steering vector, the above formulation may break down when $\mathbf{A}$ contains the real steering vector of SOI. This happens when the presumed look direction is erroneous.

To amend this drawback, we generalize the above formulation by mainlobe control. The direction of SOI is assumed to be contained within a spatial sector instead of a particular direction. Let $\boldsymbol{\theta}_s$ denote the spatial sector where the directions of SOI is assumed to be contained. The extension of the optimization problem (2) is given as follows:

$$\min_{\mathbf{w}} \mathbf{w}^H\mathbf{R}\mathbf{w}/2\,, \quad (7a)$$

$$\text{subject to } \mathbf{A}_s{}^H\mathbf{w} = 1\,, \quad (7b)$$

$$\|\mathbf{w}^H\mathbf{A}\|_p^p < \varepsilon, \quad (7c)$$

where $\mathbf{A}_s = \left[\mathbf{a}\left(\theta_{s,1}\right), \ldots, \mathbf{a}\left(\theta_{s,N_s}\right)\right]$ consists of possible steering vectors of SOI within the spatial sector $\boldsymbol{\theta}_s$.

The solution to the above optimization can be derived in a similar way as the derivation presented in Section II. Firstly, we combine the constraints (7b) and (7c):

$$\min_{\mathbf{w}} \mathbf{w}^H\mathbf{R}\mathbf{w}/2 \quad (8a)$$

$$\text{subject to } \| \mathbf{\Gamma}^H\mathbf{w} - \mathbf{d}^*\|_p^p, \quad (8b)$$

where $\mathbf{\Gamma} = [\mathbf{A}|\alpha\mathbf{A}_s]$. Next, we formulate the Lagrange function and equate its gradient to zero. Finally, the weight vector update equation is obtained as follows:

$\mathbf{w}(i+1)=$

$$\tilde{\lambda}\left(\mathbf{R} + \tilde{\lambda}\mathbf{\Gamma}\boldsymbol{\Pi}\left(\mathbf{w}(i)\right)\mathbf{\Gamma}^H\right)^{-1}\mathbf{\Gamma}\boldsymbol{\Pi}\left(\mathbf{w}(i)\right)\mathbf{d}^*, \quad (9)$$

where $\boldsymbol{\Pi}(\boldsymbol{w})$ is given by $\boldsymbol{\Pi}(\boldsymbol{w}) = \text{diag}\{|(\mathbf{\Gamma}^H\mathbf{w} - \mathbf{d}^*)_1|^{p-2}, \ldots, |(\mathbf{\Gamma}^H\mathbf{w} - \mathbf{d}^*)_N|^{p-2}\}$.

It is worth mentioning that the matrix $\mathbf{\Gamma}$ can be implemented by considering only a few directions representing the directions of the SOI within the spatial sector $\boldsymbol{\theta}_s$. In fact, the number of directions within $\boldsymbol{\theta}_s$ can be as small as two, i.e. $N_s = 2$. To do so, the first direction $\theta_{s,1}$ is taken at the left boundary while the other $\theta_{s,2}$ is taken at the right boundary. It is demonstrated by computer simulations that the optimization problem (7), compared to optimization problem (2), has several advantages: 1) better robustness against look direction mismatch; 2) smaller value of N to generate $\mathbf{A}$ with respect to interference directions; 3) better performance when the real interference directions are not precisely located at the sampling directions of $\mathbf{A}$.

IV. IMPLEMENTATION OF THE PROPOSED ALGORITHMS

From (7) and (10), it is observed that there are three parameters: p, λ, and γ, impacting the performance of the proposed beamformers. The parameter p determines the sparsity of the beampattern. The smaller the value of p, the sparser the derived beampattern (or equivalently, the lower the sidelobe level). The parameter λ determines the effectiveness of the sparse constraint. Using a large λ emphasizes the impact of the sparse constraint and will result in a trivial solution $\mathbf{w}$ ($\mathbf{w} = \mathbf{0}$ gives the smallest value of $\|\mathbf{w}^H\mathbf{A}\|_p^p$), since the constraint on distortionless response in (2b) and (7b) will be neglected in this situation. Similarly, using a large γ emphasizes the impact of the distortionless response constraint and will attenuate the effect of the sparse constraint. Therefore, these parameters should be chosen properly in order to have good compromise between suppression of interferences and maintenance of the desired source.

In order to appropriately choose λ, we compute the gradient of (3) with respect to λ, and equating it to zero yields

$$\| \bar{\mathbf{A}}^H\mathbf{w} - \mathbf{d}^*\|_p^p = 0. \quad (10)$$

Left multiplying (5) with $\mathbf{w}^H$ yields

$$\mathbf{w}^H\mathbf{R}\mathbf{w} + \tilde{\lambda}\bar{\mathbf{A}}\boldsymbol{\Pi}(\boldsymbol{w})(\bar{\mathbf{A}}^H\mathbf{w} - \mathbf{d}^*) = 0. \quad (11)$$

With the definition of $\bar{\mathbf{A}}$ and $\mathbf{d}$, we may equivalently express (10) as

$$\| \mathbf{A}^H\mathbf{w}\|_p^p + \alpha^p|\mathbf{w}^H\mathbf{a}(\theta_0) - 1|^p = 0. \quad (12)$$

Also, (11) is equivalent to

$$\mathbf{w}^H\mathbf{R}\mathbf{w} + \| \mathbf{A}^H\mathbf{w}\|_p^p + \alpha^p\mathbf{w}^H\mathbf{a}(\theta_0) |\mathbf{w}^H\mathbf{a}(\theta_0) - 1|^{p-2}(\mathbf{w}^H\mathbf{a}(\theta_0) - 1) = 0, \quad (13)$$

which can be written as

$$\mathbf{w}^H\mathbf{R}\mathbf{w} + \| \mathbf{A}^H\mathbf{w}\|_p^p + \alpha^p|\mathbf{w}^H\mathbf{a}(\theta_0) - 1|^p + \alpha^p|\mathbf{w}^H\mathbf{a}(\theta_0) - 1|^{p-2}(\mathbf{w}^H\mathbf{a}(\theta_0) - 1) = 0. \quad (14)$$

With (12), (14) can be simplified as

$$\mathbf{w}^H\mathbf{R}\mathbf{w} + \alpha^p|\mathbf{w}^H\mathbf{a}(\theta_0) - 1|^{p-2} (\mathbf{w}^H\mathbf{a}(\theta_0) - 1) = 0. \quad (15)$$

Solving (15) gives the solution of λ as

$$\lambda = \gamma\left(\frac{\mathbf{w}^H\mathbf{R}\mathbf{w}}{|\mathbf{w}^H\mathbf{a}(\theta_0) - 1|^{p-2}(\mathbf{w}^H\mathbf{a}(\theta_0) - 1)}\right)^{1-p}. \quad (16)$$

When implementing the algorithm, we may alternatively update $\mathbf{w}(i)$ and $\lambda(i)$ or $\gamma(i)$ using (6) and (16), respectively. For the second algorithm, the relationship between λ and γ is the same as (16) by replacing $\bar{\mathbf{A}}$ with $\mathbf{\Gamma}$, and setting the denominator as $\|\mathbf{A}_s^H\mathbf{w} - \mathbf{d}\|^{p-1}$.

Because we have deduced the relationship between λ and γ, we may properly determine one of them and compute the other one using (16). Based on the existing literature, when p is fixed, some principles of choosing a proper λ, such as the L-curve [13], have been introduced. Therefore, when implementing the algorithm, we may firstly choose a proper value of p. Then, we use existing principles to determine λ. When λ is derived, we use (16) to compute γ. It should be emphasized that how to precisely choose λ is still an open issue. Current algorithms do not guarantee the optimal results. Fortunately, from our computer simulations, we see that the proposed algorithms are not sensitive to the choice of λ and γ. Therefore, they can be chosen empirically. When doing so, we should keep in mind that if a large λ

or a small p is used, the value of γ should not be too small so that a trivial $\mathbf{w}$ can be avoided.

We summarize the proposed algorithms in Table 1.

Table 1: Summary of the proposed algorithms

Step 1: Parameter setting: 1) Set up p, λ and γ (λ and γ can be chosen empirically); 2) Generate $\bar{\mathbf{A}}$ according to the presumed look direction and sidelobe sector;
Step 2: Initialize: i=0, $\mathbf{w}(0)$;
Step 3: Iterations: 1) Compute $\boldsymbol{\Pi}(\mathbf{w}(\mathrm{i}))$; 2) Update $\mathbf{w}(\mathrm{i})$ using (6) or (9); 3) If λ is not chosen empirically, using the L-curve principle to determine λ; 4) Compute γ using (16); 5) i=i+1;
Step 4: Terminate the algorithm if the stopping criterion is satisfied, otherwise go to *Step 3*.

The stopping criterion can be chosen as $i>N_{iter}$, where N_{iter} is a preset number. The other usually adopted stopping rule is to evaluate the value of $\|\mathbf{w}(i+1)-\mathbf{w}(i)\|_2^2/\|\mathbf{w}(i)\|_2^2$. If it is smaller than a preset threshold, terminate the algorithm.

V. COMPUTER SIMULATIONS

In this section, computer simulations are conducted to verify validity and advantages of the proposed algorithms. In all the simulations, the beampattern is computed by $20\log_{10}|\mathbf{w}^H\mathbf{a}(\theta)|$ for $\theta\in[-90^o,90^o]$.

A. Implementation of algorithm I to array synthesis

It is observed that the proposed algorithms can also be applied to the array synthesis algorithm [14] with **R**=**I** in (2). The sparse constraint (2c) plays a role to suppress the assigned sidelobe sector. To verify this, we conduct the following simulations. A uniform linear array (ULA) with 32 half-wavelength spaced sensors is assumed.

Firstly, we assume sidelobe suppression sector as$[-90^o,-1^o]\cup[1^o,90^o]$. The array beampattern obtained using the proposed algorithm is shown in Fig. 1.

One can see from Fig. 1 that the proposed algorithm reduces the sidelobe level several decibels from the original beampattern. Also, it is noticed that the smaller the value of p, the greater the sidelobe suppression. This coincides with our previous analysis that p controls the sparsity of the beampattern.

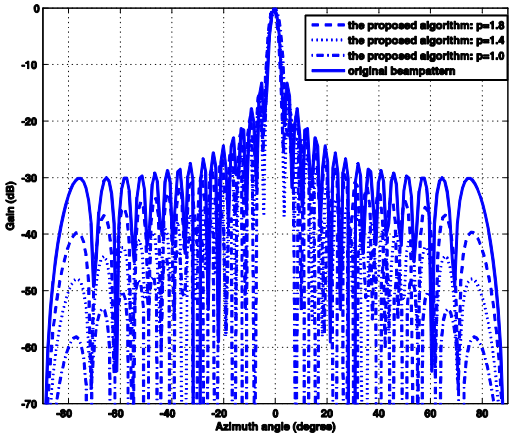

Fig. 1. Array beampatterns for a 32-sensor ULA with sidelobe suppression sector $[-90^o,-1^o]\cup[1^o,90^o]$.

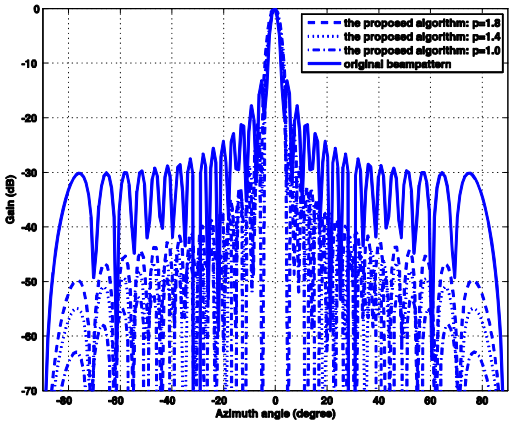

Fig. 2. Array beampatterns for a 32-sensor ULA with sidelobe suppression sector $[-90^o,-5^o]\cup[5^o,90^o]$.

In certain applications, one may like to maintain the mainlobe of the array response at a certain width to ensure that the signal coming from the desired look direction will be received by the array with sufficient array gain. In Fig. 2, the proposed algorithm is used in the design of array pattern under this situation. The sidelobe suppression sector is chosen to be $[-90^o,-5^o]\cup[5^o,90^o]$.

It is seen that compared with the original beampattern, the beamwidth is increased slightly, while the sidelobe level is improved by the order of tens of decibels. The sidelobes beside the mainlobe is significantly improved by more than 5 dB.

B. Evaluation of algorithm I on narrowband beamforming

In this section, a ULA with eight half-wavelength inter-element spaced sensors is used. The DOA of the desired signal is supposed to be 0^o, and the DOAs of three interferences are set to -30^o, 30^o and 70^o. The signal-to-noise ratio (SNR) is set to 10 dB, and the signal-to-interference ratio (SIR) is -20 dB. 100 snapshots are used to compute the covariance matrix **R**. The regularization parameter λ is set to 0.2 in all the simulations. The matrix A consists of array steering vectors in the angular range from $[-90^o, -1^o] \cup [1^o, 90^o]$ with 1^o sampling interval. In this case, all the potential interferences are contained in **A** and the sidelobe level of the whole angular range is under control.

In the first simulation, we assume mismatch does not occur. The proposed method is compared with the MVDR beamformer. With different p and α, the derived beampatterns are shown in Fig. 3.

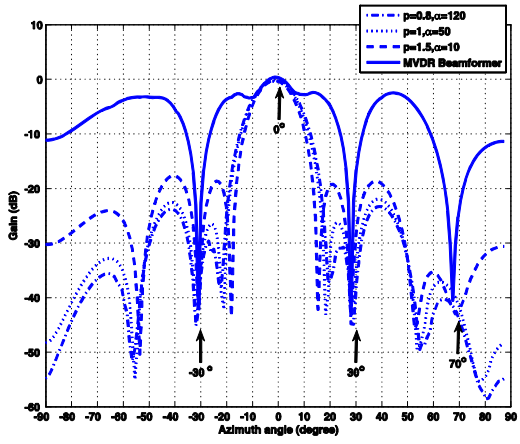

Fig. 3. Array beampatterns for SNR=10 dB in the no mismatch case (Algorithm I).

It is observed that all of the beamformers cast deep nulls in directions of interference and generate distortionless response at the look direction. However, the sidelobe level of the MVDR beamformer is much higher than that of the proposed algorithm. For the proposed beamformer, the sidelobe level decreases as p decreases. This is because the smaller the p, the smaller the values of the beampattern are. This simulation result coincides with our previous analysis.

Figure 4 shows the plots of output SINR versus SNR with 1000 independent trials. The output signal to interference plus noise ratio (SINR) is calculated via

$$SINR_{output} = \frac{\sigma_s^2 \mathbf{w}^H \mathbf{a}(\theta_0)\mathbf{a}^H(\theta_0)\mathbf{w}}{\mathbf{w}^H \left(\sum_{j=1}^{J} \sigma_j^2 \mathbf{a}(\theta_j)\mathbf{a}^H(\theta_j) + \sigma_n^2 \mathbf{I}\right)\mathbf{w}}, \quad (17)$$

where J denotes the number of interferences.

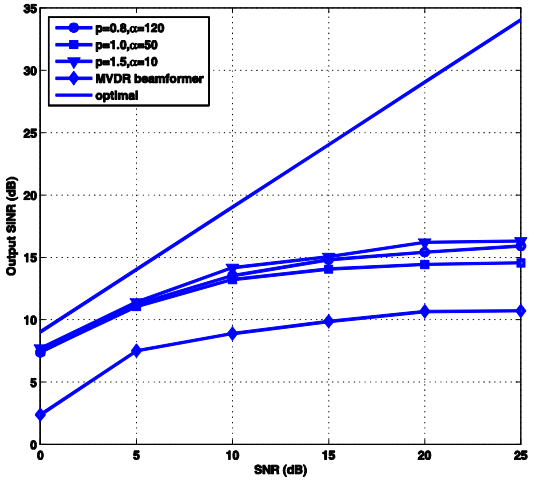

Fig. 4. Plots of output SINR versus SNR in the no mismatch case (Algorithm I).

It is noted that the proposed beamformer can achieve an output SINR approximately 6 dB larger than that of MVDR beamformer for all of the SNRs. For different p and α, the proposed algorithm shows similar performance results.

In the second simulation, we assume there is a 3^o mismatch in the look direction. The desired signal impinges the array from broadside, while the look direction of the beamformer is assumed to be 3^o. Figure 5 shows the obtained beampatterns of different algorithms.

It is observed from Fig. 5 that the MVDR beamformer introduced a deep null at 0^o, which means the desired source is suppressed due to imprecise knowledge of the look direction. In contrast, the proposed beamformer only slightly

shifts its maximum point of the beampattern, and is still capable of generating a distortionless response at the direction of SOI. At interference directions, all the algorithms are able to cast deep nulls.

Figure 6 plots the output SINR versus SNR with 1000 independent trials. From the figure, we see that the performance of MVDR beamformer and the proposed one differ a lot. It is observed that the proposed algorithm gives an output SINR about 10 dB, while the MVDR beamformer fails to work in all the cases. Similar to Figure 4, for different p and α, the proposed algorithm has very similar performance.

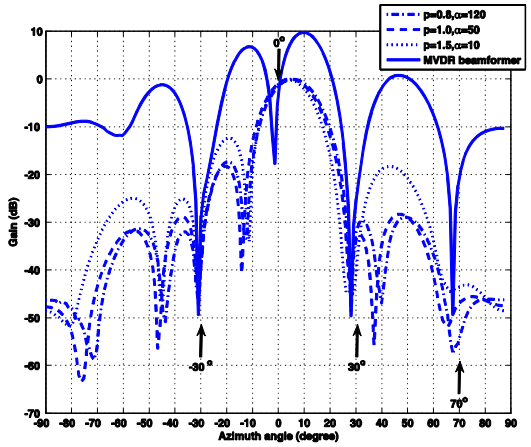

Fig. 5. Array beampatterns for SNR=10 dB with 3° mismatch (Algorithm I).

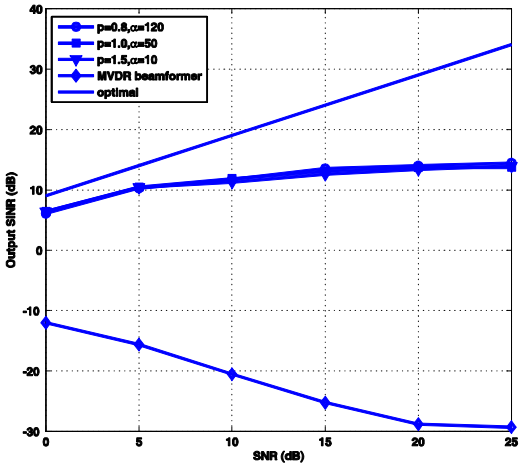

Fig. 6. Plots of output SINR versus SNR with 3° mismatch (Algorithm I).

C. Evaluation of algorithm II on narrowband beamforming

In this section, we evaluate the performance of the proposed Algorithm II when directions of interferences and the SOI are not precisely known. An ULA with ten half-wavelength inter-element spaced sensors is used. The actual source DOA is supposed to be 0°, and the DOAs of four interference signals are set to -30°, -10°, 20° and 45°. The SIR is assumed to be -20 dB, and the SNR is assumed to be 10 dB. The matrix $\mathbf{A}$ consists of array steering vectors in the DOA range $[-90^o,-4^o) \cup (4^o,90^o]$with 10° sampling interval, while the matrix $\mathbf{A}_s$ consists of only two array steering vectors that is defined at -3° and 3°.

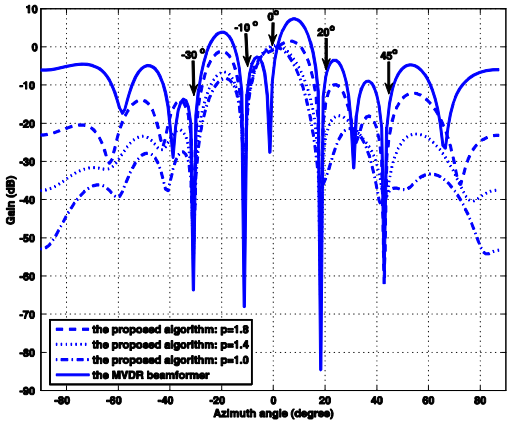

Fig. 7. Array beampatterns for SNR=10 dB with 3° mismatch (Algorithm II).

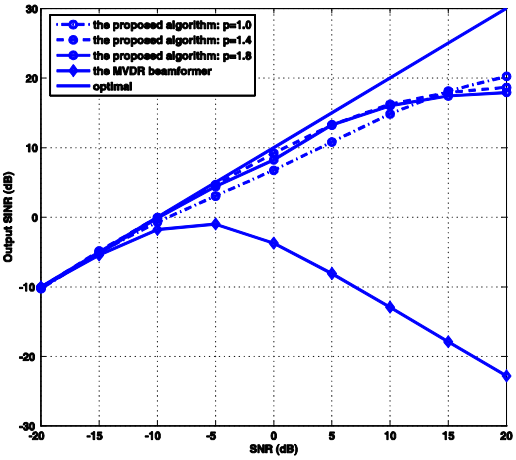

Fig. 8. Plots of output SINR versus SNR with 3° mismatch (Algorithm II).

Note that unlike the simulation settings in the previous section, we greatly relax our interferences constraints by using a 10^o sampling interval. Also, the interference from 45^o is not located on the spatial sampling grid.

In the first simulation, we assume a 3^o look mismatch, i.e., the SOI impinges the array from broadside direction, while we assume it comes from 3^o. Figure 7 shows the derived beampatterns using different algorithms.

It is observed from Fig. 7 that the MVDR castsa deep null at 0^o, while the proposed algorithm still performs satisfactorily in this case. For interference directions, the algorithm casts deep nulls.

Figure 8 plots the output SINR versus SNR for 1000 independent trials. We see that the proposed algorithm outperforms the MVDR beamformer. The MVDR beamformer almost fails to work in all the cases. The proposed algorithms with different values of p again achieve similar performance to each other.

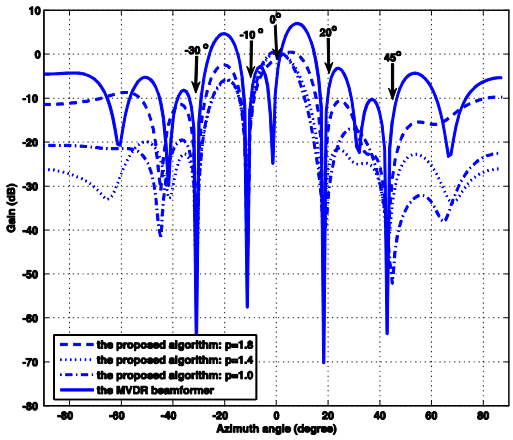

Fig. 9. Array beampatterns for SNR=10 dB with 3^o mismatch and sensor position error (Algorithm II).

In the second simulation, besides the look direction mismatch, we further assume sensor position error which is a Gaussian variable with zero mean and standard deviation 0.1 times the sensor spacing appears in the steering vector. Figure 9 depicts the obtained beampatterns using different algorithms. Figure 10 shows the output SINR versus SNR for 1000 independent trials.

From Fig. 9, we see that the proposed algorithm is capable of maintaining distortionless response at the direction of the SOI, while the MVDR beamformer suppresses the SOI about 25 dB in order to yield a distortionless response at the look direction. Figure 10 clearly demonstrates that the proposed algorithm is robust against look direction error and sensor position error, while the MVDR beamformer is very sensitive to these errors.

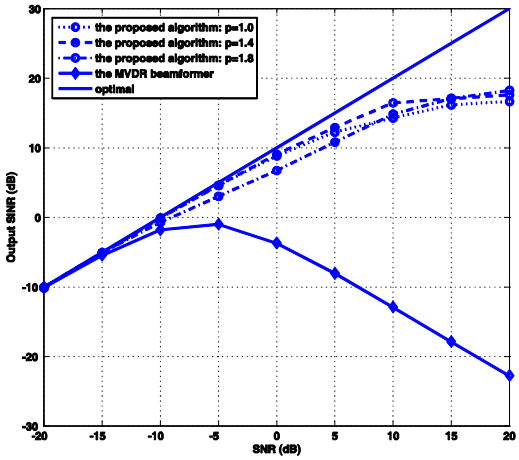

Fig. 10. Plots of output SINR versus SNR with 3^o mismatch and sensor position error (Algorithm II).

VI. CONCLUSIONS

In this paper, we propose two beamforming algorithms which use sparse constraint to suppress a sidelobe level of beampattern. Taking imperfect array into account, we also add robust constraint on the new beamformers. All these algorithms are easy to implement. Computer simulations demonstrate that these algorithms work satisfactorily in the presence of steering vector error. Furthermore, the proposed algorithms are not very sensitive to the values of parameters used in the algorithms.

ACKNOWLEDGMENT

The authors would like to express their gratitude to all the anonymous reviewers for their comments and suggestions to improve the quality of the paper.

REFERENCES

[1] J. Capon, "High resolution frequency wavenumber spectrum analysis," *Proceedings*

of the IEEE, vol. 57, no. 8, pp. 1408-1418, August 1969.

[2] M. Wax and Y. Anu, "Performance analysis of the minimum variance beamformer," *IEEE Transactions on Signal Processing*, vol. 44, no. 4, pp. 928-937, April 1996.

[3] H. Cox, "Resolving power and sensitivity to mismatch of optimum array processors," *Journal of the Acoustic Society of America*, vol. 54, no. 3, pp. 771-785, September 1973.

[4] J. Li and P. Stoica, *Robust Adaptive Beamforming*, New York: Wiley, 2006.

[5] J. L. Krolik, "The performance of matched-field beamformers with mediterranean vertical array data," *IEEE Transactions on Signal Processing*, vol. 44, no. 10, pp. 2605-2611, 1996.

[6] K. Buckley, and L. Griffths, "An adaptive generalized sidelobe canceller with derivative constraints," *IEEE Transactions on Antennas and Propagations*, vol. 34, no. 3, pp. 311-319, March 1986.

[7] A. K. Steele, "Comparison of directional and derivative constraints for beamformers subject to multiple linear constraints," *IEE Proceedings F Communications, Radar and Signal Processing*, vol. 130, no. 1, pp. 41-45, 1983.

[8] M. H. Er, B. P. Ng, and A. Cantoni, "A new set of constraints for derivative-constrained broad-band beamformers," *Journal of Electrical and Electronics Engineering*, vol. 11, no. 2, pp. 87-101, June 1991.

[9] J. Li, P. Stoica, and Z. Wang, "Doubly constrained robust capon beamformer," *IEEE Transactions on Signal Processing*, vol. 52, no. 9, pp. 2407-2423, September 2004.

[10] A. N. Tikhonov, and Y. V. Arsenin, *Solution of Ill-posed Problems*, V. H. Winston and Sons, 1977.

[11] A. B. Gershman, "Robust adaptive beamforming in sensor arrays," *AEU-International Journal of Electronics and Communications*, vol. 53, no. 6, pp. 305-314, June 1999.

[12] K. Harmanci, "Relationships between adaptive minimum variance beamforming and optimal source localization," *IEEE Transactions on Signal Processing*, vol. 48, no. 1, pp. 1-13, 2000.

[13] B. D. Rao, K. Engan, S. F. Cotter, and J. Palmer, and K. K. Delgado, "Subset selection in noise based on diversity measure minimization," *IEEE Transactions on Signal Processing*, vol. 51, no. 3, pp. 760-770, March 2003.

[14] L. J. Griffths and K. M. Buckley, "Quiescent pattern control in lineary constrained adpatively arrays," *IEEE Transactions on Acoustics, Speech and Signal Processing*, vol. 35, no. 7, pp. 917-926, July 1987.

Ying Zhang received the B.Eng. degree and Ph.D. degree in Electronics Engineering (EE) from the University of Electronic Science and Technology of China (UESTC) and Nanyang Technological University (NTU) in 2004 and 2010, respectively. Since 2010, she has been a research fellow at the School of Electrical & Electronic School (EEE), NTU. Her research interests include array signal processing, sparse signal representation, and wireless communication.

Huapeng Zhao received the B.Eng. degree and M.Sc. degree in EE from UESTC in 2004 and 2007, respectively. Since 2008, he has been working towards his Ph.D. degree in NTU. His research interests include computational electromagnetics, statistical electromagnetics, signal processing techniques in electromagnetics, and measurements in electromagnetic reverberation chamber.

Joni Polili Lie received the Ph.D. degree in EE from NTU in 2009. He is currently a research scientist in Temasek Labs@NTU. His research interests include array signal processing and wireless communications.

Boon Poh Ng received the B.Eng. degree in Electrical Engineering from Nanyang Technological Institute, Singapore, in 1987, the D.I.C. and M.Sc. degrees in Communications and Signal Processing from Imperial College, University of London, London, U.K., in 1991, and the Ph.D. degree from NTU, Singapore, in 1995.

He is currently an Associate Professor at the School of EEE, NTU. His research interests include array synthesis, adaptive array processing, spectral estimation, and digital signal processing in general.

Qun Wan received the B.Sc. degree in Applied Physics from Nanjing University, China, in 1993. He received the M.Sc. and Ph.D. degrees in EE from UESTC, China, in 1996 and 2000, respectively. From 2001 to 2003, he was a post-doctor with Department of EE, Tinghua Univeristy, China.

He is currently a professor at the College of EE, UESTC. His research interests include mobile localization, spectral estimation, sparse signal processing, and array signal processing.